AN ANALYSIS OF DIRECT ION-MOLECULE REACTIONS

Bruce H. Mahan

Department of Chemistry, and Inorganic Materials Research Division of the Lawrence Berkeley Laboratory, University of California, Berkeley, California 94720

One of the major goals of the study of molecular collision phenomena is to learn how to analyze or anticipate the dynamics of an elementary reaction without engaging in extensive numerical calculations. This is of particular importance in ion-molecule chemistry, where often the reaction dynamics are affected by more than one potential energy surface. The accurate calculation of these surfaces, and their use to investigate the exact classical collision dynamics, while highly edifying, can be quite expensive and time consuming. It is of interest, therefore, to explore the efficacy with which simple models for the reaction process can be used to understand and predict the energy and angular distributions of products, isotope effects, and total reaction cross sections.

It has proved convenient to describe the dynamic mechanism of an elementary bimolecular chemical reaction as involving either a short-lived, direct interaction of collision partners, or a long-lived collision complex. In the former case, the collision partners are close (within approximately an equilibrium bond distance) for a time comparable to a vibrational period, but less than a full rotational period. In the latter case, the partners are close and strongly

interacting for several rotational periods. The dividing line between the two classifications can be hazy, and it is also unrealistic to believe that a reaction can proceed exclusively via a long-lived collision complex. Examples of ion-molecule reactions which fall in each extreme classification are now known (for reviews and references to the original literature, see Dubrin and Henchman, 1972 and Mahan, 1974). Examples of intermediate behavior have also appeared (Chiang, Gislason, Mahan, and Werner, 1971, and Mahan and Sloane, 1973).

For reactions which proceed through a long-lived collision complex, the interaction between all atoms may be strong enough so that the accessible phase space of the complex is explored fairly uniformly. In these cases, we can hope that the statistical or phase space theories of chemical reaction can reproduce and predict such things as the relative yields of products, isotope effects, and energy partitioning. The effectiveness of the present forms of statistical theory is still an open question, however.

For reactions which proceed by a direct interaction mechanism, there is also a relatively simple model available: the classical trajectory calculation with Monte Carlo sampling of a properly weighted set of initial conditions. As mentioned above, this approach can be expensive, and can produce more information than can be readily assimilated. In this paper we shall use a simple sequential impulse model to analyze the dynamics of direct ion-molecule reactions.

The experimental studies which have prompted this analysis have been largely concerned with exoergic or thermoneutral hydrogen atom transfer reactions. To illustrate the nature of these findings we shall summarize some of the recent results obtained for the $O^+(H_2,H)OH^+$ reaction (Gillen, Mahan, and Winn, 1973 abc).

Direct Hydrogen Atom Transfer Processes

Figure 1 shows the velocity vector distribution of OH^+ from the $O^+(H_2,H)OH^+$ reaction as measured in ion beam scattering experiments. This distribution has features which are quite characteristic of the results obtained for a number of exoergic hydrogen atom transfer reactions. The results are displayed by plotting contours of constant intensity in a polar coordinate system which has an origin which moves at the velocity of the center-of-mass of the collision partners. Thus the radial coordinate gives the speed of OH^+ relative to the centroid of the O^+-H_2 system. Small values of the radial coordinate correspond to small values of the final relative translational energy of the products, and therefore, by energy conservation, to large product internal excitation. The large labeled circles give the locations of two values of Q, the translational exoergicity. By energy conservation, Q can be written as

$$Q \equiv \frac{\mu'(g')^2}{2} - \frac{\mu g^2}{2} = -\Delta E_o^o - U \qquad (1)$$

Here μ is the reduced mass and g is the relative speed of

the products (primed) and reactants (unprimed), ΔE_o^o is the internal energy change for the reaction, and U is the internal excitation energy of the products.

For reactions in which the products are an atom and a molecule in their ground electronic states, Q is bounded by the situations in which U is zero or to D, the dissociation energy of the molecule:

$$-\Delta E_o^o - D \leq Q \leq -\Delta E_o^o. \qquad (2)$$

The lower limit can be violated (apparently) if either product is in an excited electronic state, and the simplest way to take this into account is to recognize that for such processes, ΔE_o^o has a different value (Gillen, Mahan, and Winn, 1973a). For the $O^+(H_2,H)OH^+$ reaction,

$$-4.5 \leq Q \leq +0.43 \text{ eV},$$

and the Q circles in Fig. 1 correspond closely to these limits. In effect, these circles define a "stability zone" for OH^+ in its ground electronic state.

The angular coordinate θ in Fig. 1 measures the direction of the OH^+ product relative to the direction of the O^+ projectile. Thus for a direct interaction process, it is a qualitative (and eventually quantitative) representation of the force exerted between collision partners. Product OH^+ found in the small angle ($\theta \leq 45°$) region in Fig. 1 was formed in a way such that the net integrated force between products was small during the collision. By analogy with

elastic scattering of structureless particles, this implies formation of the products in the small angle region is by grazing collisions. In a similar manner, we conclude that in the formation of products at large scattering angles, large forces are involved, and these are associated with nearly head-on collisions between reactants. By using the impulse model of direct reactions, we hope to delineate what is meant by grazing and head-on collisions more clearly.

Figure 1 shows that there is a strong maximum in the intensity of OH^+ at the spectator stripping velocity: a scattering angle of zero degrees and a speed relative to the centroid consistent with the general expression

$$u = u_o \left(\frac{A}{A+B}\right) \left(\frac{C}{B+C}\right) \qquad (3)$$

which applies to the reaction A(BC,C)AB. In Eq. (3) the letters represent the masses of the atoms, and u and u_o are respectively the product and projectile speeds relative to the centroid. Appearance of OH^+ at the spectator stripping velocity implies that the reaction occurred with no net integrated force on the freed hydrogen atom. With one exception, all exoergic hydrogen transfer reactions so far investigated have displayed a very prominent intensity maximum at or very near the spectator stripping velocity. The exception is apparently the ground state reaction $Kr^+(H_2,H)KrH^+$, which may also be unique in having a potential energy barrier between reactants and products (Henglein, 1972). Unfortunately, the stripping peak is frequently so prominent that reactions

have often been rather carelessly described as "stripping processes", and the large angle scattering ignored or dismissed as unimportant. Without question, the idea that atom B can be transferred to A with no force being exerted on C is quite remarkable. It is therefore of considerable interest to determine in detail how this can occur, and how important it is to the overall chemical reaction cross section.

The experimental determinations of the final relative energy distributions of reaction products have been somewhat limited by the low velocity resolution employed so far. However, in most of the cases investigated, it is qualitatively clear that in the intermediate to high range of initial relative energies (>3 eV), the products in the small angle region are somewhat more excited internally than the products scattered through large angles. In this energy regime, much or most of the internal excitation of the products is supplied by the initial translational energy of the reactants. In the nearly head-on collisions which lead to large angle scattering, the large forces that occur provide the mechanism for disposing of some of this incipient product excitation as relative translational energy. There is less possibility for this disposal in the grazing collisions which produce the very small angle scattering. A more quantitative expression of these ideas is possible in terms of the sequential impulse model. as we shall see.

In the regime of high initial translational energy, the total reaction cross section is greatly influenced by the

problem of stabilizing the product molecule against dissociation. This can be illustrated most clearly for the product formed at the spectator stripping velocity. The Q-value for this product is

$$Q_{ss} = -\frac{B}{A+B} \qquad (4)$$

where E is the laboratory energy of the projectile ion A. If E is made large enough, Q_{ss} will become more negative than the lower limit given by Eq. (2), and the molecular product in its ground electronic state will be unstable. In the early work which demonstrated the importance of spectator stripping in the reactions of Ar^+, N_2^+, and CO^+ with H_2, it was anticipated (Henglein, 1966) that the intensity peak at small angles would be lost entirely when E reached the critical value

$$E_C = \left(\frac{A+B}{B}\right)(\Delta E_o^o + D) \qquad (5)$$

at which the internal energy of the stripped molecular product exceeds its dissociation energy. However, it was observed that for these systems, the forward scattered peak is not lost at high initial relative energies, but instead decreases in intensity and moves to speeds greater than the spectator stripping value. That is, some of the forward scattered molecules are stabilized by recoil which can evidently occur in grazing collision in these systems.

One reaction has been found that displays the loss of forward scattered products at initial energies above the critical value for spectator stripping. Figure 2 shows the

velocity vector distribution of OH^+ from the $O^+(H_2,H)OH^+$ reaction at an initial relative energy of 11.1 eV. At this energy, the spectator stripping velocity (indicated by a small cross) lies in the zone where OH^+ in its electronic ground state is unstable. Indeed, the intensity peak so evident at lower initial relative energies (cf. Fig. 1) has been lost. Thus, the potential energy surface for the $O^+(H_2,H)OH^+$ reaction lacks the features which allow stabilization by product recoil in the small angle region. It would be valuable to know what these critical features are, and in addition, to be able to understand the occurrence of the intensity peaks located at approximately 45° in Fig. 2. We shall find that the sequential impulse model illuminates this problem considerably.

The Sequential Impulse Model

A number of simple models for the atom transfer process have been proposed, and at least partially tested against molecular beam scattering data (Bates, Cook, and Smith, 1964; Light and Horrocks, 1964; Suplinskas, 1968; Kuntz, 1970; Chang and Light, 1970; Hierl, Herman, and Wolfgang, 1970; George and Suplinskas, 1971; Grice and Hardin, 1971; Marron, 1973). Even allowing for the necessity of using extremely simple approximations to potential energy surfaces and mechanical behavior, most of these models are lacking in generality or rigor, and some have not been particularly illuminating. The sequential impulse model proposed by Bates,

Cook, and Smith (1964) is conceptually simple, and has the capacity for considerable refinement. In brief, the reaction A(BC,C)AB is viewed as an event in which A hits B impulsively and elastically, B then hits C in a like manner, and A then combines with B if their energy of relative motion is less than the dissociation energy of the product molecule. Suplinskas (1968) and George and Suplinskas (1971) have elaborated the model, and have shown that it can reproduce the major features of the Ar^+-D_2 reactive scattering. Gillen, Mahan, and Winn (1973c) found that a version of the model in which the atoms interact via hard sphere potentials is consistent with the distributions of the products of the reaction of O^+ with D_2 and HD in the regime of high relative energies. These two sets of applications involved calculation of the final product velocities from sampled initial conditions using large digital computers. However, to better discern and analyze the nature of the collisions which give products at various scattering angles and speeds, it would be valuable if the product distributions could be expressed analytically and evaluated with a small calculator. This proves to be possible, and the results will be reported in detail elsewhere. In what follows we shall demonstrate that a number of conclusions can be drawn from the model merely by using velocity vector diagrams.

First, let us review some fundamental features of elastic collisions which are essential to the development and understanding of the sequential impulse model. Consider atom A

moving with an initial laboratory velocity $\underset{\sim}{V}_1$ toward atom B, which is initially stationary in the laboratory. The initial relative velocity $\underset{\sim}{g}$ is equal to $\underset{\sim}{V}_1$, and the velocity of the center-of-mass of the A-B system is $\underset{\sim}{V}_1\ A/(A+B)$. Regardless of the nature of the two body collision, the center-of-mass velocity is unchanged. Since the collision is assumed to be elastic, the final and initial relative velocity vectors have the same magnitude, but different direction. The final relative velocity vector is obtained by rotating the initial vector about the fixed center-of-mass velocity. The result, as is shown in Fig. 3, is that the final laboratory velocity $\underset{\sim}{V}_1'$ of particle A is a vector which terminates on a sphere of radius $V_1\ B/(A+B)$ centered at the centroid velocity. Similarly, $\underset{\sim}{V}_2'$, the final laboratory velocity of B, lies on a concentric sphere of radius $V_1\ A/(A+B)$.

The scattering angle χ_1, measured in the center-of-mass system of A and B, is also shown in Fig. 3. From the geometry, it is clear that the bisector of $\underset{\sim}{V}_2'$ passes through the centroid velocity, and bisects the angle χ_1. As a result, we can write

$$V_2' = 2\ \frac{A}{A+B}\ V_1\ \sin\left(\frac{\chi_1}{2}\right) \qquad (6)$$

for the magnitude of V_2'. This relation and the construction used to find it will be particularly useful later.

The vector relations just discussed give the possible values of the particle velocities after an elastic collision. The distribution of intensity is also important, and is expressed

most compactly by the classical differential scattering cross section $I(\chi)$, where for a monotonic potential

$$I(\chi) = \frac{b}{\sin\chi \left|\frac{d\chi}{db}\right|} . \qquad (7)$$

Here b is the aiming error or impact parameter. To evaluate $I(\chi)$, the relation between b and χ must be found from the intermolecular potential function. For hard spheres, the result is particularly simple:

$$I(\chi) = \frac{d^2}{4} \qquad (8)$$

where d is the mutual collision diameter. Thus for this model, the scattered intensity is independent of χ. For more realistic potentials, $I(\chi)$ is large at small angles and drops rapidly as χ increases. In the range of angles from 60-180°, $I(\chi)$ decreases rather slowly, and in the large angle region, is pretty well represented by a constant term characteristic of hard sphere scattering. The hard sphere differential cross section is therefore a good first approximation to the intensity distribution, particularly for high energies and large scattering angles.

There is another feature of high energy collisions that is of importance. Such collisions, particularly those that produce large angle scattering, are impulsive. That is, the time during which a large force is exerted between a pair of atoms is small compared to the natural frequencies for nuclear motion in molecules. For example, if atoms repell each other according to the potential

$$\phi = \phi_0 e^{-r/L},$$

where L is a range parameter, then the force is greater than 10% of its maximum value for a period of 3τ, where τ is a characteristic collision time defined by

$$\tau = 2L/g.$$

During this time, the relative velocity changes from approximately 90% of its initial value to 90% of its final value. For typical values of L and energies in the electron-volt range, τ is of the order of 2×10^{-15} sec. This is shorter than the vibrational period, and much shorter than the rotational period of H_2. Thus for the case of a high energy atom A hitting a diatomic molecule BC, it often may be quite reasonable to describe the process as an elastic collision between A and B, followed by an independent elastic collision between B and C. The initial condition for the second condition is, of course, the final state of the first collision.

The primary object of a model for the reaction process is to calculate the intensity of scattered product AB as a function of the scattering angle θ and speed relative to the center-of-mass of the ABC system. Evaluating the intensity as a function of $\underset{\sim}{V}_3''$, the final velocity in the laboratory system of the free atom C, is completely equivalent to this, since by momentum conservation, each value of $\underset{\sim}{V}_3''$ corresponds to a definite value of θ and the final relative speed. Finding the magnitude of $\underset{\sim}{V}_3''$ is a simple matter if one knows χ_1 and χ_2, the scattering angles for the A-B and

B-C collisions in their individual center-of-mass coordinate systems. As indicated above, the magnitude of the laboratory velocity of atom B after the A-B collision is

$$V_2' = 2 \frac{A}{A+B} \sin(\frac{\chi_1}{2}).$$

Now we simply regard V_2' as the initial velocity for the B-C collision, and apply the analogous formula to get

$$V_3'' = 4(\frac{A}{A+B})(\frac{B}{B+C}) \sin(\frac{\chi_1}{2}) \sin(\frac{\chi_2}{2}). \qquad (9)$$

Having found the laboratory velocity of atom C after a particular sequence of impulses, we must ask whether or not this constitutes a reactive collision. Our criterion for reaction is the simplest possible: the value of V_3'' must lie in the stability zone which corresponds to the internal energy of AB being less than its dissociation energy. This is an important approximation, since it allows us to disregard details of the trajectories such as the possibility of additional collisions between C and B or A. However, it is probably a good approximation, since for high energy collisions, the size of the cross section is governed largely by product stability considerations. Moreover, hard sphere trajectory calculations (Gillen, Mahan, and Winn, 1973b) have demonstrated the relative unimportance of additional impulses and other details of the trajectories, and also the effectiveness of this reaction criterion in reproducing experimental data. However, the approximation does restrict application of the model to reactions where the potential energy surface has very

simple properties: thermoneutral or nearly so, and no substantial wells or barriers.

Equation (9) suggests that a variety of impulse sequences can contribute to the product intensity at $\underset{\sim}{V}_3''$. The angle χ_1 may be large or small, as long as χ_2 has the appropriate small or large value consistent with the selected value of $\underset{\sim}{V}_3''$. However, there are limits to the range of χ_1 and χ_2 values that can be involved, and these limits are connected with the direction of $\underset{\sim}{V}_3''$, a property which we have not yet used.

To see how this limitation comes about, consider Fig. 4. Here we treat only those values of $\underset{\sim}{V}_2'$ which lie in the plane defined by the vectors $\underset{\sim}{V}_1$ and $\underset{\sim}{V}_3''$. As indicated earlier, the possible values of $\underset{\sim}{V}_2'$ lie on a circle of radius $V_1\, A/(A+B)$ centered on $\underset{\sim}{V}_1$ at this distance from the origin of the laboratory coordinate system. The locus of all B-C center-of-mass velocities in this plane plays a very important role. It can be found by multiplying all possible $\underset{\sim}{V}_2'$ vectors by the factor $B/(B+C)$, and plotting the points. The result is a circle of radius

$$R = \left(\frac{A}{A+B}\right)\left(\frac{B}{B+C}\right) V_1 \qquad (10)$$

centered on V_1 at a distance R from the laboratory origin. Let us call this the centroid circle.

Now consider an arbitrary centroid velocity for the B-C system just before (and after) their collision. These centroids must be on the centroid circle, and must also lie on the perpendicular bisector of $\underset{\sim}{V}_3''$. As Fig. 4 shows, there are just

two centroids which satisfy both these conditions for any given $\underset{\sim}{V}_3''$ vector. One of these corresponds to a large χ_2 (and small χ_1), the other to the values of χ_1 and χ_2 being interchanged. These two angles are the extreme values of χ_1 and χ_2 that are consistent with a selected $\underset{\sim}{V}_3''$.

The origin of the intermediate values of χ_1 and χ_2 becomes obvious if we recognize that $\underset{\sim}{V}_2'$ need not lie in the plane of $\underset{\sim}{V}_1$ and $\underset{\sim}{V}_3''$. Thus the centroid circle is really part of a centroid sphere of radius R, and the perpendicular bisector of $\underset{\sim}{V}_3''$ is a plane. The intersection of this bisecting plane with the centroid sphere is a circle - the "magic circle" - perpendicular to the $\underset{\sim}{V}_1$-$\underset{\sim}{V}_3''$ plane. As one moves along the magic circle, all the χ_1-χ_2 pairs that can contribute to scattering at $\underset{\sim}{V}_3''$ are encountered. Thus the product intensity at $\underset{\sim}{V}_3''$ can be found by summing the properly weighted contributions of all allowed χ_1-χ_2 scattering pairs.

For the present purposes, the details of this weighted summation are not needed, but it is useful to note that the distribution over the various χ_1-χ_2 pairs is nearly uniform. The departure from uniformity comes about because the angle α between $\underset{\sim}{V}_2'$ and the BC internuclear axis is distributed with a weighting factor of $\sin\alpha$. Consequently, the BC axis is more likely to lie perpendicular to $\underset{\sim}{V}_2'$ than parallel. As a result, impact parameters for the B-C collision have a relatively high probability of being near their maximum allowed value of r_0, the BC equilibrium bond distance. Thus smaller values of χ_2 are more probable than larger

values, in contrast to the usual situation for hard sphere scattering. However, while this can affect the details of the product velocity distribution, it is not important in determining the gross features of the distributions with which we are concerned here.

A number of qualitative conclusions can be drawn directly from Fig. 4. First, there will be certain $\underset{\sim}{V}_3''$ vectors for which the perpendicular bisector does not intersect the centroid sphere. Even though these values of $\underset{\sim}{V}_3''$ might be consistent with the total energy and momentum conservation laws, they can not be produced by a sequence of two elastic impulses. For example, events in which $\underset{\sim}{V}_3''$ is directed at 180° in the laboratory coordinate system can not occur. Thus, there can be no backward recoil of particle C, and no corresponding forward recoil of the AB product.

A little reflection shows that this forward recoil could occur if, just before the A-B impulse, the vector $\underset{\sim}{V}_1$ were increased in magnitude with the center-of-mass velocity held fixed. This could occur in a real system if there were an attractive potential between reactants, and this is in fact the mechanism for forward product recoil proposed in the so-called modified stripping model (Herman, Kerstetter, Rose, and Wolfgang, 1967). In addition, one can see that forward recoil could occur if, just prior to the B-C collision, the vector $\underset{\sim}{V}_2'$ were increased in length, so that this collision would appear to be super-elastic. This could come about if there were a repulsive energy release between B and C as the products separate. This is the basic idea involved in

the so-called direct interaction with product repulsion (DIPR) model for reaction dynamics (Kuntz, 1970; Marron, 1973). The sequential impulse model thus clarifies the validity of either reactant attraction or product repulsion as sources of forward recoil.

It is evident that $\underset{\sim}{V}_3''$ vectors directed at angles other than 180° are accessible only if the magnitude of V_3'' is small enough so that there is an intersection of the bisecting plane and the centroid sphere. The condition for such an intersection can be found readily from the analytic geometry of the vector construction. The maximum values of V_3'' lie on a curve given by

$$\frac{(V_3'')_{max}}{2R} = \cos\varepsilon + 1 \qquad (11)$$

where ε is the angle between $\underset{\sim}{V}_3''$ and $\underset{\sim}{V}_1$. Equation (11) represents a cardioid which has a cusp at the origin of the laboratory velocity coordinate system. There is a corresponding cardioid which gives the maximum values of the velocity of the AB product in the center-of-mass system, and this is illustrated in Fig. 5. The minimum values of the AB product velocity are just those given by the requirement that the excitation energy of the product AB must be less than its dissociation energy. Thus the zone in velocity space that is allowed is bounded from the inside by the stability circle, and from the outside by the limiting cardioid.

The size of the limiting cardioid is proportional to R, and thus scales with V_1. However, the size of the stability

circle is determined by the magnitude of Q_{min}, a fixed number independent of V_1. Thus the size of the kinematically allowed zone can be represented as a function of initial relative energy by one cardioid, if the units of the diagram are changed as the energy changes. However, in this case there is a different sized stability circle for each initial relative energy, as indicated in Fig. 5. As the initial relative energy increases, the diameter of the stability circle increases, and eventually it intersects the limiting cardioid at the cusp. This corresponds to reaching the critical projectile energy above which products formed by spectator stripping are unstable. As the initial relative energy is increased still further, increasing amounts of the accessible small angle scattering region pass into the unstable zone, and the outline of the product distribution assumes a crescent-like shape. The experimentally observed distributions for the O^+-H_2 and O^+-D_2 reactions have just this shape when the initial relative energy is in the 11-30 eV range. Moreover, the observed decrease of the total reaction cross section with increasing energy can be in large measure attributed to the concomitant diminution of the size of the product stability zone.

The considerations just outlined provide an explanation of why the spectator stripping peak and all small angle scattering is lost at high energy in the $O^+(H_2,H)OH^+$ reaction, but is stabilized by forward recoil in the reactions of N_2^+, CO^+, and Ar^+ with H_2 and D_2. In the O^+-H_2 case, the reaction

is only slightly exoergic (ΔH = -0.43 eV) and there is no obvious mechanism for producing large amounts of forward recoil. In contrast, the reactions of N_2^+, CO^+, and Ar^+ are notably more exoergic ($\Delta H \cong$ -1.4 eV). If all of this exoergicity were to be released as product repulsion in some of the grazing collisions, forward recoil and product stabilization could occur, as is observed.

Having delineated the general limits and energy dependence of the product velocity vector distribution predicted by the sequential impulse model, we can now turn to some of the details of the intensity variations. From Fig. 4 it is evident that $\underset{\sim}{V}_3''$ vectors of small magnitude directed approximately perpendicular to $\underset{\sim}{V}_1$ will have bisecting planes which intersect the centroid sphere to generate magic circles of large radii. There is, therefore, a relatively large range of χ_1-χ_2 pairs which can produce these events. The intensity in the small angle scattering region will thus be large if the initial relative energy is low enough to place the small angle scattering region in the stability zone. As V_3'' increases in magnitude, the size of the magic circle decreases, and the product intensity goes down.

In order to see this effect develop systematically, in Fig. 6 we have plotted the χ_1-χ_2 pairs that produce scattering at various fixed values of the product scattering angle θ. The calculations apply to the $O^+(D_2,D)OD^+$ reaction at an initial relative energy of 20 eV, a situation in which the very small angle scattering does not lie in a stable region

of velocity space. The solid lines refer to products formed with the minimum allowed Q value of -5 eV (the correct value, if the exoergicity is ignored), while the dotted lines correspond to a Q value of -1 eV.

Figure 6 exposes the reason for the intensity maximum observed experimentally near $45° \leq \theta \leq 60°$. For this region, the range of χ_1-χ_2 pairs that can produce stable products reaches a maximum. At smaller values of θ, the range of allowed χ_1-χ_2 pairs drops abruptly, and the observed product intensity does also. At values of θ greater than 90°, the allowed range of χ_1-χ_2 pairs again diminishes, and the expected and observed product intensities diminish.

Notice that the values of χ_1 and χ_2 which produce large values of θ are themselves large. This is consistent with the idea that backscattered products do come from nearly head-on collisions. In order to have <u>both</u> χ_1 and χ_2 large, A must hit B nearly head-on, and B must hit C in a like manner. This implies a nearly collinear ABC conformation at the beginning of the collision. Similarly, we can see that the values of χ_1 and χ_2 which contribute to small values of θ are of modest magnitude (~35-90°). Thus it is moderately accurate to associate the region of small θ with "grazing" collisions, although in some of the events that contribute, substantial deflections of A by B or of B by C do occur. It is probably better to think of $\theta < 15°$ as the grazing collision region.

Figure 6 also shows that the range of χ_1-χ_2 pairs that can produce scattering at Q = -1 eV is smaller at any value

of θ than the corresponding range for $Q = -5$ eV. Moreover, the χ_1-χ_2 pairs for a given value of θ lie at slightly larger values for $Q = -1$ eV than for $Q = -5$ eV. Thus, principally because of a smaller allowed range of χ_1-χ_2 pairs, the intensity of the lesser internally excited products will be less than that of the more excited products. In other words, there is an intrinsic tendency for the internal energy distribution of the products to be inverted.

So far we have discussed the detailed events in which A hits η, and B has a hard sphere collision with C. In order for such events to occur, the angle α between $\underline{v}_2'$ and the BC internuclear axis must be less than $\pi/2$. For $\alpha > \pi/2$, there will be no B-C collision, and thus no force on C. If the AB product of these events is stable, it has the velocity calculated from the spectator stripping model. Thus, if A, B, and C are treated as hard spheres, spectator stripping comes largely from events in which A strikes and combines with the second atom it sees as it approaches BC. Stripping processes are also possible for values of α somewhat smaller than $\pi/2$ if the mutual hard sphere diameter of the B-C pair is less than the impact parameter of the second collision. In the limit of vanishing hard sphere diameter for B and C, all collisions will be spectator stripping processes.

These considerations help to make clear why spectator stripping is so prominent in the product velocity vector distributions of ion-molecule reactions. If the potential

energy surfaces for these reactions have only a weak dependence on the ABC angle, then trajectories are possible in which the projectile A strikes and combines with the second atom without exerting force on the free or spectator atom. Moreover, if there are strong attractive forces between A and B, but not between B and C, there will be trajectories of the stripping type even when α is significantly less than $\pi/2$. Note that if spectator stripping is described as involving grazing collisions, it is the B-C interaction, and not necessarily the A-B collision which is of the grazing type.

Spectator stripping resembles both the rainbow and glory effects in atomic elastic scattering (Bernstein, 1966). Like rainbow scattering, it appears that there is in the reactive situation a range of initial conditions (in this case, the angle α) which gives product scattered at or very near to one point in velocity space. The fact that this point is at a scattering angle of zero degrees is also significant, since just as in glory scattering, there is an integration over all values of the azimuthal angle which is performed by the detector only when θ equals zero degrees. These two factors and the relatively low apparatus resolution employed so far combine to give spectator stripping a fame which it perhaps does not fully deserve. After considering realistic potential energy surfaces, it is very difficult to accept the fact that B and C can separate with a truly zero force between them. In the future, when product distributions are examined with high resolution, some or all of the spectator peaks may be found not at $\theta = 0°$, but at small but finite scattering angles.

Even now it should be realized that to go from the intensity contour maps of Figs. 1 and 2 to actual total reaction cross sections, one must apply a weighting factor of $\sin\theta$, and then integrate the intensity over angle and speed. Thus, product at $\theta = 0°$ is given zero weight, and that near $\theta = 90°$ contributes most heavily to the total reaction cross section. In other words, most of the chemistry is done by the type of events described at least approximately by the sequential impulse model.

Acknowledgement: This work was supported by the U. S. Atomic Energy Commission. Discussions with Dr. John S. Winn and Dr. Keith T. Gillen contributed significantly to the formulation of the ideas developed here.

REFERENCES

Bates, D. R., Cook, C. J. and Smith, F. J. (1964). Proc. Phys. Soc. 83, 49.

Bernstein, R. B. (1966). Advances in Chemical Physics, 10 (Ed. J. Ross). John Wiley and Sons, New York.

Chang, D. T. and Light, J. C. (1970). J. Chem. Phys. 52, 5687.

Chiang, M. H., Gislason, E. A., Mahan, B. H., Tsao, C. W. and Werner, A.S. (1971). J. Phys. Chem. 75, 1426.

Dubrin, J. and Henchman, M. J. (1972). MTP International Review of Science Series I, 9, 213 (Ed. J. C. Polanyi). Butterworth and Co., London.

George T. F. and Suplinskas, R. J. (1971). J. Chem. Phys. 54, 1037.

Gillen, K. T., Mahan, B. H. and Winn, J. S. (1973a). J. Chem. Phys. 58, 5373.

Gillen, K. T., Mahan, B. H. and Winn, J. S. (1973b). Chem. Phys. Lett. 22, 344.

Gillen, K. T., Mahan, B. H. and Winn, J. S. (1973c). J. Chem. Phys. 59, 6380.

Grice, R. and Hardin, D. R. (1971). Molecular Physics, 21, 805.

Henglein, A. (1966). Advan. Chem. Ser. 58, 63.

Henglein, A. (1972). J. Phys. Chem. 76, 3883.

Herman, Z., Kerstetter, J., Rose, T. and Wolfgang, R. (1967). Disc. Faraday Soc. 44, 123.

Hierl, P. M., Herman, Z. and Wolfgang, R. (1970). J. Chem. Phys. 53, 660.

Kuntz, P. J. (1970). Trans. Faraday Soc. 66, 2980.

Light, J. C. and Horrocks, J. (1964). Proc. Phys. Soc. 84, 527.

Mahan, B. H. (1974) MTP International Review of Science, Series II, 9, (Ed. D. R. Herschbach). Butterworth and Co., London.

Mahan, B. H. and Sloane, T. M. (1973). J. Chem. Phys. 59, 5661.

Marron, Michael T. (1973). J. Chem. Phys. 58, 153.

Suplinskas, R. J. (1968). J. Chem. Phys. 49, 5046.

FIGURE CAPTIONS

Figure 1. A contour map of the specific intensity of OH^+ formed by the $O^+(H_2,H)OH^+$ reaction at an initial relative energy of 5.56 eV. The radial coordinate is the speed of OH^+ relative to the center-of-mass of the entire system. The angular coordinate measures the deflection in the center-of-mass system, of the OH^+ from the original direction of the O^+ projectile. The spectator stripping velocity is indicated by a small cross.

Figure 2. A contour map of the specific intensity of OH^+ formed from collisions at 11.1 eV initial relative energy. Note the absence of an intensity peak at 0° and the appearance of peaks at ±60°. The spectator stripping velocity, marked by a small cross, lies inside the Q = -4.5 eV circle, where OH^+ in its ground state is unstable.

Figure 3. A velocity vector diagram for the elastic collision of atom A with atom B. The circles marked V_1' and V_2' are, respectively, the loci of all possible final laboratory velocity vectors for atoms A and B. The scattering angle in the center-of-mass system is designated by χ. Note that the perpendicular bisector of any V_2' vector bisects χ and passes through the A-B centroid velocity.

Figure 4. A velocity vector diagram for the sequential impulse model in the plane of the initial projectile velocity V_1, and the final velocity of atom C, V_3''. The large Q circles indicate a part of the stability zone for the reaction: the velocity of atom C must lie in this zone if AB is to be stable to dissociation.

Figure 5. The cardioid which gives the maximum velocities of OD^+ from the $O^+(D_2,D)OD^+$ reaction according to the sequential impulse model. The maximum velocity of OD^+ according to overall energy conservation is the Q = 0 circle. The three smaller circles give the minimum velocity of OD^+ consistent with product stability (i.e., the Q = -5 eV limit) for the three values of the initial relative energy indicated.

Figure 6. The χ_1-χ_2 pairs that contribute to the intensity at various values of the product scattering angle θ for the reaction $O^+(D_2,D)OD^+$ at 20 eV initial relative energy. The solid lines pertain to product at Q = -5 eV, the dashed lines to product at Q = -1 eV.

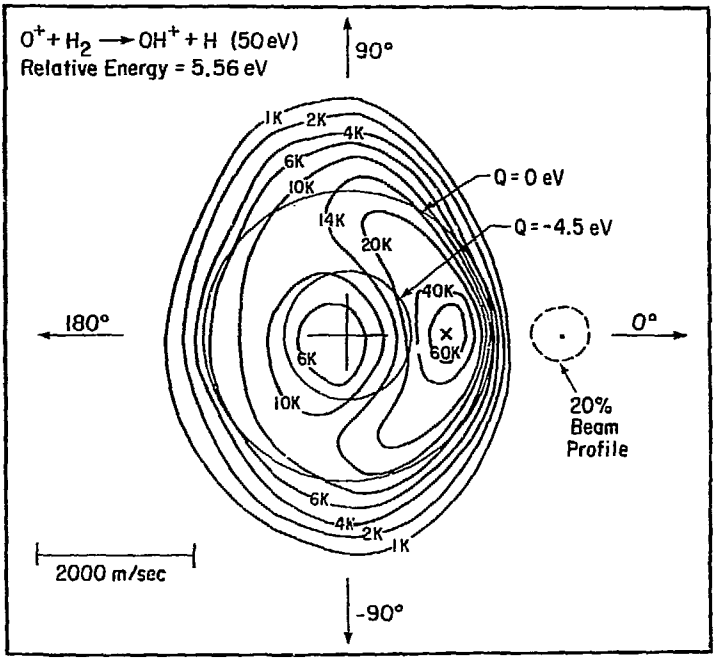

XBL727-6538

Fig. 1

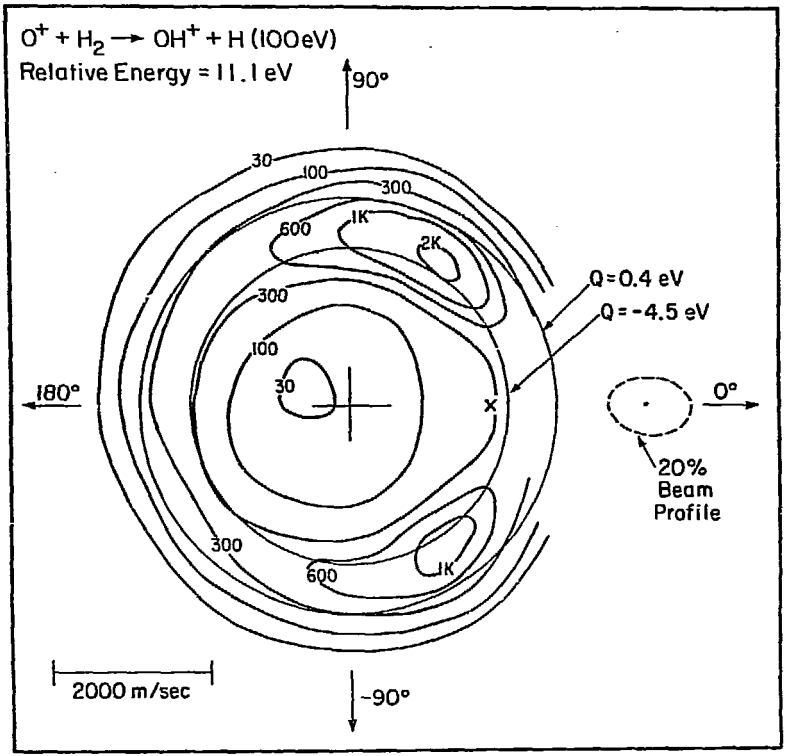

XBL 727-6541

Fig. 2

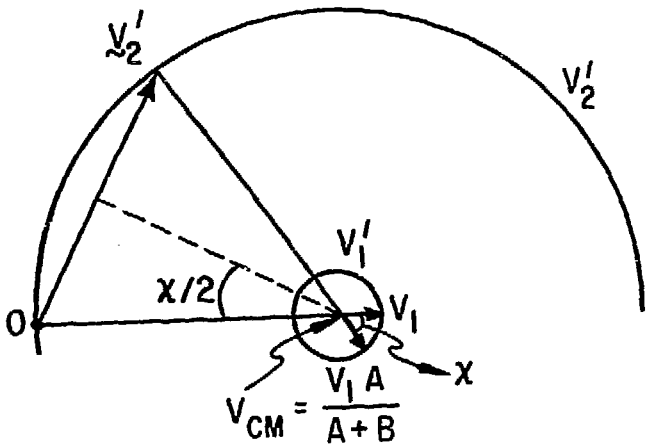

XBL 748-7055

Fig. 3

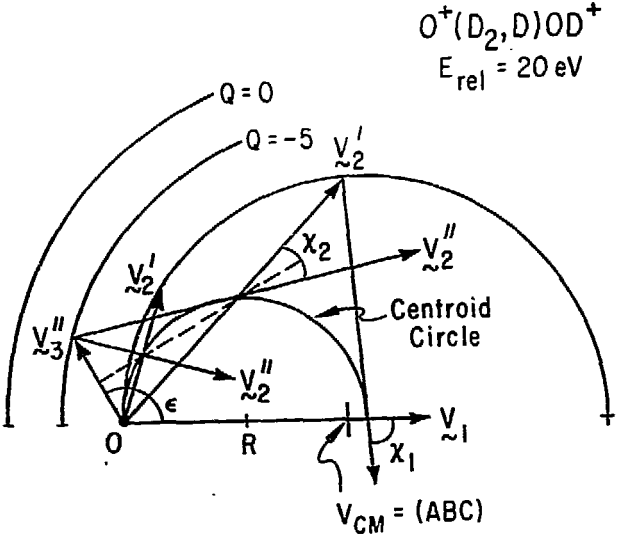

XBL 748-7056

Fig. 4

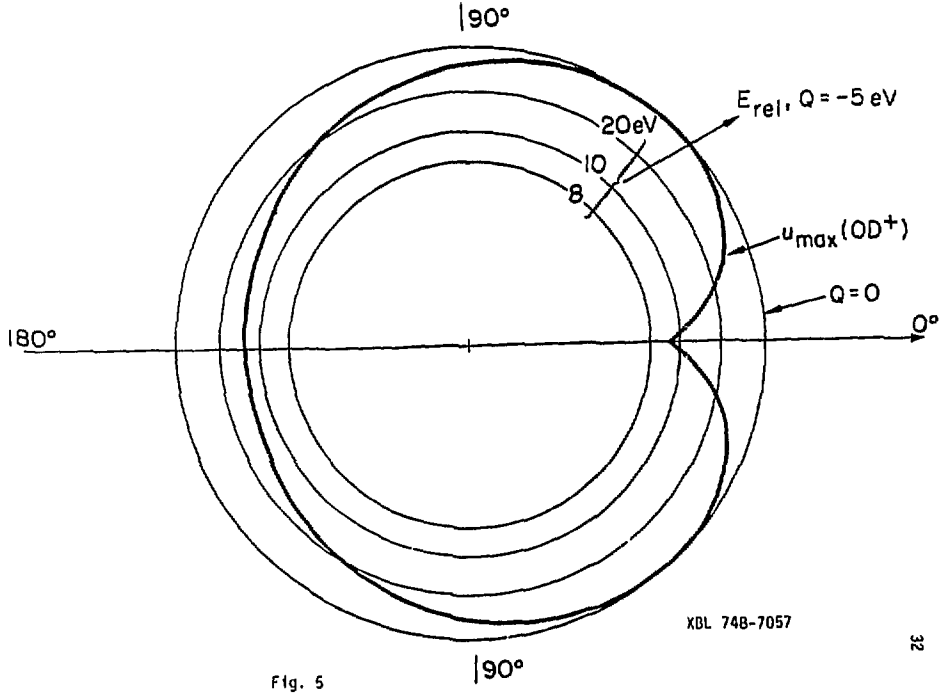

XBL 748-7057

Fig. 5

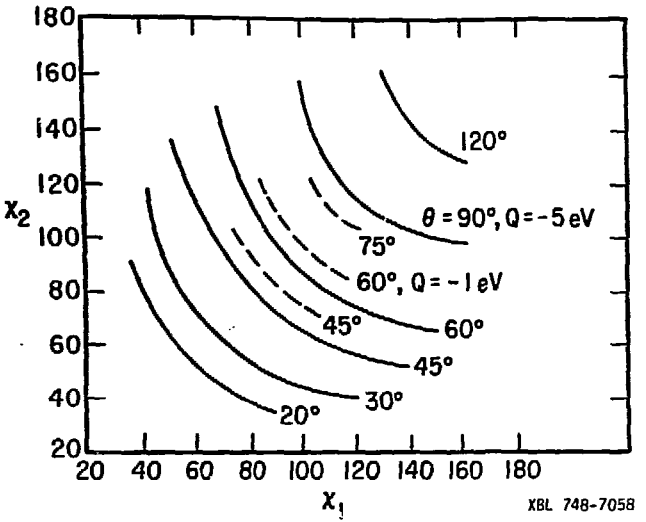
180
160
140
120
100
80
60
40
20
X_2
20 40 60 80 100 120 140 160 180
X_1
120°
θ = 90°, Q = -5 eV
75°
60°, Q = -1 eV
45°
60°
45°
30°
20°
XBL 748-7058

Fig. 6